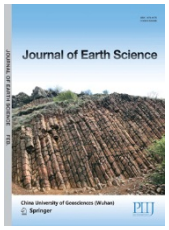

Journal of Earth Science
地球科学学刊(英文版)
ISSN 1674-487X,CN 42-1788/P

《Journal of Earth Science》网络首发论文

题目： Joint Effects and Spatiotemporal Characteristics of the Driving Factors of Landslides in Earthquake Areas

作者： Jintao YANG，Chong XU，Xu JIN

网络首发日期： 2021-04-07

引用格式： Jintao YANG，Chong XU，Xu JIN. Joint Effects and Spatiotemporal Characteristics of the Driving Factors of Landslides in Earthquake Areas ． Journal of Earth Science. https://kns.cnki.net/kcms/detail/42.1788.P.20210407.1418.004.html

Published online：2021-04-07 14:38:49
URL：https://kns.cnki.net/kcms/detail/42.1788.P.20210407.1418.004.html

https://doi.org/10.1007/s12583-021-1465-4

Joint Effects and Spatiotemporal Characteristics of the Driving Factors of Landslides in Earthquake Areas

- **Jintao YANG[1,2], Chong XU[3*], Xu JIN[4]**

[1]State Key Laboratory of Resources and Environmental Information System, Institute of Geographic Sciences and Natural Resources Research, Chinese Academy of Sciences, Beijing 100101, China

[2]University of Chinese Academy of Sciences, Beijing 100049, China

[3]National Institute of Natural Hazards, Ministry of Emergency Management of China, 100085, Beijing, China

[4]Chengdu Yuanjing Technology Co., Ltd. Chengdu 610094, China

*** Correspondence:**

Chong XU

chongxu@ninhm.ac.cn

Abstract

Understanding the joint effects of earthquakes and driving factors on the spatial distribution of landslides is helpful for targeted disaster prevention and mitigation in earthquake-prone areas. By far, little work has been done on this issue. This study analyzed the co-seismic landslide of the MS 8.0 Wenchuan earthquake in 2008 and 2014. The joint effects and spatiotemporal characteristics of the driving factors in seismic regions were revealed. Results show that a) between 2008 and 2014, the dominant driving-factor for landslides has changed from earthquake to rock mass. b) driving factors with weak driving force have a significant enhancement under the joint effects of other factors. c) the joint effects of driving factors and earthquake decays with time. The study concluded that the strong vibration of the Wenchuan earthquake and the rock mass strength are the biggest contributors to the spatial distribution of landslides in 2008 and 2014, respectively. It means that the driving force of the earthquake is weaker than that of the rock mass after six years of the Wenchuan earthquake. Moreover, the landslide spatial distribution can attribute to the joint effects of the Wenchuan earthquake and driving factors, and the earthquake have an enhanced effect on other factors.

Keywords: Geodetector, co-seismic landslide, spatial pattern, triggering factors, interaction effects, driving force

1 Introduction

Earthquakes are the main triggering factor of landslides (Huang, 2007, Xu and Xu, 2021). China is an earthquake-prone area, in 2019, there were more than 30 earthquakes of magnitude 5 or above in China (www.cea.gov.cn/cea/index). Furthermore, China's mountainous area accounts for 69.1% of total land area(Sheng, 1959),the rolling terrain of mountainous area creates a good breeding environment for the landslide. The combination of frequent earthquakes and mountain topography provide good prerequisites for landslides, pose a huge threat to the lives and properties in mountainous areas (Dai et al., 2002, Marano et al., 2010). Understanding the joint effects of the earthquake and geographical conditions on the spatial distribution of landslides is helpful for making targeted disaster prevention and reduction strategies. However, the joint effects have not been fully studied, and the spatiotemporal characteristics of these joint effects have not been fully revealed.

The spatial distribution of landslides is attributed to many driving factors such as geomorphology factors, geotechnical properties, and hydrological conditions (Achour et al., 2017, Hadji et al., 2017, Mahdadi et al., 2018, Anis et al., 2019). These factors reflect the natural conditions of landslides, and were taken as the basic driving factors for regional landslide assessment (Fan et al., 2012, Xu et al., 2012, Xu et al., 2012, Hadji et al., 2013). Many methods have been used to explore the relationship between driving factors and landslides. For example, correlation matrix, multiple linear and non-linear regression model, logistic regression, frequency ratio, weights of evidence, analytic hierarchy process, information value(Hadji et al., 2013, Achour et al., 2017, Hadji et al., 2017, Karim et al., 2018, Mahdadi et al., 2018, Manchar et al., 2018, Anis et al., 2019). Besides, machine learning or deep learning methods are also used to predict the potential for landslides(Lee et al., 2020, Yao et al., 2020), but deep

learning methods usually are not possible to know the contribution of driving factor due to the black box algorithms. In these studies, the joint effects of driving factors are rarely considered. However, landslides are the result of the joint effects of driving factors (Wang et al., 2018).

In addition to the driving factors that reflect the natural conditions of landslides, triggering factors are another important factor affecting the spatial distribution of landslides. Mainly triggering factors include earthquakes (Zhao et al., 2014, Xu C. et al., 2015, Fan et al., 2019), rainfall (Hadji et al., 2013, Wang et al., 2015, Vargas-Cuervo et al., 2019), volcanoes (Che et al., 2011), and human activities (Mendes et al., 2018, Persichillo et al., 2018). Driving factors have different effects on landslides under the influence of different triggering factors (Pantelidis, 2011, Tang, 2015), due to tremendous changes in the environment of geological disasters (Lin et al., 2004, Lin et al., 2006). Research shown that soft and loose solid material is prone to mudslides under heavy rainfall (Furuichi et al., 2018), and steep slopes are easier to collapse and cast under shaking of earthquakes(XU and Huang, 2008). Moreover, the threshold of rainfall for debris flow decreased in Beichuan and Mianyuan River basin after the MS 8.0 Wenchuan earthquake (Tang et al., 2009, Yuanjing et al., 2013). That means the contributions of driving factors were changed under the effect of triggering factors. It is worth noting that the direct-action time of triggering factors is usually short, consequently, the joint effect of the triggering factors and the driving factors also changes with the triggering factors. However, the spatiotemporal characteristics of these changes were rarely considered.

Two important issues are not addressed well in studying the driving factors of landslide. First, the joint effects of driving factors are not fully considered. Second,

the spatiotemporal characteristics of the joint effects are unclear. The aims of this study are: a) to clarify the joint effects of driving factors and triggering factors on the spatial distribution of landslides; and b) to reveal the spatiotemporal characteristics of the joint effects of triggering factors and driving factors after a major earthquake.

2 Data and Methods

2.1 Methods

GeoDetector is a spatial statistical method to measure the spatial stratification heterogeneous of a geographical phenomenon and to reveal the driving force behind the geographical phenomenon(Wang and Hu, 2012, Wang et al., 2016). It is widely used in natural sciences, social sciences, environmental sciences and human health. The core idea is based on the assumption that if a geographical phenomenon (eg, the spatial distribution of landslides) is affected by driving factors (eg, rock mass, earthquake, rainfall), then the spatial stratification heterogeneity of the geographical phenomenon can be identified by the driving factors or the interactions of the driving factors(Wang et al., 2010). GeoDetector includes 4 Sub-detectors: factor detector, interaction detector, risk detector, and ecological detector. The factor detector is mainly used to detect potential factors that cause a certain geographical phenomenon (Wang and Xu, 2017). The interaction detector is used to detect the joint effect of multiple factors on geographical phenomena. The risk detector is used to detect the risk level of a certain geographical phenomenon in different categories of a driving factor.

The factor detector was used to detect the driving factors that have a significant impact on the landslide spatial distribution, and to determine their driving forces (DF). The principle of the factor detector is as follows:

$$DF = 1 - \frac{1}{N\sigma^2}\sum_{w=1}^{m} N_w \sigma_w^2, \quad DF \in [0,1] \qquad (1)$$

More detailed of Equation (1) is as follows:

$$DF = 1 - \frac{1}{N\sigma^2}\sum_{w=1}^{m} N_w \sigma_w^2 = 1 - \frac{\sum_{w=1}^{m}\sum_{j=1}^{N_w}(\gamma_{w_j} - \overline{\gamma_w})^2}{\sum_{i=1}^{N}(\gamma_i - \overline{\gamma})^2} = 1 - \frac{SSW}{SST} \qquad (2)$$

Where the sum of squares within is

$$SSW = \sum_{w=1}^{m}\sum_{j=1}^{N_w}(\gamma_{w_j} - \overline{\gamma_w})^2 \qquad (3)$$

and the total sum of squares is

$$SST = \sum_{i=1}^{N}(\gamma_i - \overline{\gamma})^2 \qquad (4)$$

Where N is the number of mapping units in the study area (the number of grid or pixel in the study area). Specifically, taken kernel density map of landslides (KDML) as the geographical phenomenon, and taken the seismic intensity as a driving factor (seismic intensity has four categories, and each category corresponds to a level), N is the number of grid (or pixel) in KDML, N_w is the grids (or pixel) number of KDML within the *w-th* category of seismic intensity, σ^2 is the variance of the KDML which is calculated by formula 4, σ_w^2 is the variance of the KDML within the *w-th* category of the seismic intensity. γ_i is the *i-th* grid (or pixel) value of KDML and $\bar{\gamma}$ is average value of the KDML. m is the number of categories of seismic intensity (the

driving factor). $\gamma_{w_j}$is the *j-th* grid (or pixel) value of the KDML within the *w-th* category of seismic intensity, and $\overline{\gamma_w}$ is the average value of KDML within the *w-th* category of seismic intensity. DF is the driving force of driving factor to the landslide spatial distribution. $0 \leq DF \leq 1$, when $DF = 0$, which indicates that this driving factor has nothing to do with the spatial distribution of landslides. The larger the value of DF is, the stronger the driving force is.

The interaction detector is used to identify the joint effects of two driving factors. This interaction detector to quantifies the joint effect by combine two driving factors A and B (e.g., by overlaying geographical layers seismic intensity and rock mass in GIS to form a new layer C). The attribute of layer C is defined as the combination of the attributes of layers A and B (Seismic Intensity and Rock Mass). The driving force (DF) of C is the joint effects of driving factors A and B. therefore, there are two steps in interaction detector when to calculate the joint effects of driving factors A and B. First, overlaying A and B to form a new layer C in GIS. Second, take layer C as the driving factor and take kernel density map of landslides (KDML) as the geographical phenomenon, then calculate the driving force of C though factor detector (factor detector was introduced above).

The risk detector is used to detect which categories of the driving factor (eg,) are at high risk and identifies whether the risk has significant differences among the categories of factor. The risk can be calculated by the average level within the w-*th* category of driving factor, its expression is as follows:

$$\bar{\gamma}_w = \frac{1}{N_w}\sum \gamma \qquad (5)$$

where γ is the value of the KDML, and $\bar{\gamma}_w$ is the average value of the KDML within the w-th category of a driving factor. The significant difference between *i-th* and *j-th* categories can be test by follows:

$$t_{\bar{\gamma}_{w=i}-\bar{\gamma}_{w=j}} = \frac{\bar{\gamma}_{w=i}-\bar{\gamma}_{w=j}}{\left[\frac{Var(\bar{\gamma}_{w=i})}{n_{w=i}}+\frac{Var(\bar{\gamma}_{w=j})}{n_{w=j}}\right]^{1/2}} \qquad (6)$$

where $\bar{\gamma}_w$ represents the mean value of KDML within the w-th category of the driving factor, n_w is the number of grids (or pixel) within the w-th category of driving factor, and Var represents the variance. Geodetector software and its principles and detailed tutorials can be downloaded for free at www.geodetector.cn.

2.2 Data

The landslide inventories of 2009 and 2014 in the study area were prepared through the visual interpretation of remote sensing images and coupled with field verification, which contain 29210 landslides in 2009 and 4841 landslides in 2014, respectively. In addition, a total of 8 driving factors were provided by the Institute of Geology, China Earthquake Administration. Among them, the driving factors include engineering rock groups, roads, settlements, DEM (Digital Elevation Model), slopes, and terrain roughness. These driving factors play an important role in the spatial distribution of landslides(Xu Chong et al., 2015). Triggering factors include earthquake intensity and precipitation, which are the main causes of landslides in this

area (Tang et al., 2009, Tang et al., 2011, Chong et al., 2014). The precipitation data was downloaded from the Data Center of the Chinese Academy of Sciences.

The landslide points in 2009 and 2014 are input into ArcMap to generate a landslide density map. In addition, the continuous factors (terrain roughness, distance to road, digital elevation model, slope, and distance to residential area) are reclassified using the ArcMap's natural breaks method (Fig. 2). Lithology is reflected by rock mass, and has five classes including harder rock group, hard rock group, soft rock group, softer rock group, and loose rock group, denoted respectively as A, B, C, D, and E. The seismic intensity can reflect the strength of the earthquake's impact on the surface or buildings. The spatial distribution of the seismic intensity in the study area was divided into 4 levels, according to the national standard GB/T 17742-2008(CEA, 2008),express as 8, 9, 10, and 11, respectively. Finally, each layer was spatially joined, and its attribute data was exported as the input data of Geodetector (GeoDetector will be introduced in the method section).

2.3 Study Area

The study area is along with the Duwen Highway in 103°14′～103°45′E and 30°54′ ～ 31°36′N. One of the China's largest urban agglomeration (Chengdu-Chongqing urban agglomeration) is adjacent to this area, which is densely populated. The area of study area is about 935 km^2, the Longmenshan fault zone crosses the study area, indicating an active tectonic setting. On May 12, 2008, the MS 8.0 Wenchuan earthquake (known as the 5.12 Wenchaun earthquake) occurred here.

The strong shaking loosened the slope structures and reduced resistance to shear stress in the soil, which increased the susceptibility of landslide. These potential risks threatened the lives and property in the affected area. Previous studies reported that secondary hazards in the study area will remain active in the future(Cui et al., 2008). Therefore, the study area is an ideal place to study the spatiotemporal characteristics and the joint effects of triggering factors and internal factors after a major earthquake, and it is valuable reference for the urban agglomerations in mountainous areas to make targeted planning decisions.

In topography, the study area gradually rises from southeast to northwest, and transitions from low to medium mountains to high mountains with altitudes from 734m to 5304m. The average slope is 36.4 degrees, and due to the steep terrain, exposed faces of slopes developed well, prone to geologic hazards such as landslides and mudslides. The climate of this area belongs to a temperate continental semi-arid monsoon climate. Due to the large elevation differences, local areas also have obvious microclimates. The annual average rainfall is between 529 ~ 1332mm, and its spatial and temporal distribution is uneven. Specifically, the rainfall is concentrated between May and September, and it in north is relatively higher than that in south. The Minjiang River is the main drainage in the study area and connects many tributaries. Precipitation is the main supply of Minjiang River during the flood season, while groundwater and melting of snow and ice are the main supplies during the dry season.

In tectonics, the study area lies in the transition zone between the southeastern margin of the Tibetan Plateau and the western Sichuan Basin. There are three major fault zones (collectively referred to as the Longmenshan fault zone) that cross the Duwen Highway in the north-east-south direction. They are the Guanxian-Jiangyou fault (also known as the Qianshan fault) and the Yingxiu-Beichuan fault (also known as the central fault) and Maowen fault (also known as Houshan fault). Among them, the Yingxiu fault is the seismogenic fault of the 2008 MS 8.0 Wenchuan earthquake. Studies have shown that secondary geological effects in the study area will enter an active stage of 10-30 years due to the Wenchuan earthquake(Cui et al., 2008).

3 Result

3.1 Changes of landslide density in different categories

The risk levels in categories of a driving factor were calculated though averaging the value of KDML within each category by risk detector (Fig. 3). From the perspective of time, the landslide density in 2009 (one year since the MS 8.0 Wenchuan earthquake) was significantly higher than that of 2014 (6 years since the MS 8.0 Wenchuan earthquake). The decreasing trend of landslide density is consistent with that of the 2005 Kashmir earthquake (Shafique, 2020). In addition, no matter in 2009 or 2014, the order of categories with high-risk to low-risk is consistent (except for factor rock mass). For example, the landslide density in categories of DEM order from high to low in 2009 is: C2> C3> C1> C4 (Fig. 3, row1; column: 1), consistent with that of 2014. That means the spatial distribution of landslides were consistent

with these driving factors. With regards to factor rock mass, landslide density in Group A is higher than that in Group B in 2009, but the landslides in Group A less than that in Group B in 2014 (Fig. 3 row: 3, column: 1). According to the thematic map of the rock mass, it is found that the area of the Group A is very small. Therefore, when the landslide density in 2014 decreased significantly, there were few landslides in Group A, which caused the landslide density in the Group A was too low in 2014.

3.2 Changes in driving force

The driving forces of driving factors to the spatial distribution of landslides were detected by the factor detector (Fig. 4). The driving forces of rock mass, roughness, slope, DEM, residential area, and road increased in order, and they are higher in 2014 than in 2009. For the two triggering factors, the driving forces of seismic intensity and precipitation in 2014 are lower than in 2009. One possible reason is the rainfall threshold of landslide is lower in 2014, which is consistent with that the earthquake decreased the rainfall threshold of mudslide(Yu et al., 2021). Factors with biggest driving forces are rock mass and seismic intensity, and they take turns to be the dominant factor in 2009 and 2014. That is inconsistent with the dominant factor of road network in the 2005 Kashmir earthquake induced landslides(Shafique et al., 2016). That is, the driving force of the MS 8.0 Wenchuan earthquake on the spatial distribution of landslides has weakened, while that of the rock mass increased.

3.3 Changes in the joint effects of driving factors

The joint effects of driving factors were detected by the interaction detector (Fig. 5). Compared with the individual driving force of a driving factor (Fig. 4), the joint effects have significantly enhanced (Fig. 5). From the perspective of time, except for the joint effects of DEM and residential area, the joint driving forces of driving factors in 2014 were stronger than in 2009. Moreover, the joint effects are all higher than the individual driving forces. Some driving factors with low driving force such as roughness and slope in Fig. 4, which have a significant enhancement with the joint effect of rock mass (Fig. 5). The strongest joint effect is the interaction of roads and rock mass, follow by the interaction of residential and rock mass. That means the interaction of human activities and geotechnical properties can be one of the main factors causing landslide.

3.4 Changes in joint effects of triggering and driving factors

The joint effects of triggering and driving factors changed significantly over time (Fig. 6). As for triggering factor earthquake, the joint effects of earthquake and driving factors in 2009 were significantly stronger than that of 2014. Moreover, the joint effects of earthquake and driving factors in 2009 were stronger than that of precipitation and driving factors. In addition, no matter in 2009 or 2014 the joint effects of earthquake and rock mass rank the top. That means the MS 8.0 Wenchuan earthquake is still play an important role in 2014. As for triggering factor precipitation,

the joint effect of precipitation and rock mass was higher than that of earthquake and slope in 2014. That means the joint effect of precipitation and rock mass can be one of the main factors causing landslide in 2014.

4 Discussion

The dominant driving factors changed from earthquake to rock mass after six years of the MS 8.0 Wenchuan earthquake. In 2009, the first year after the MS 8.0 Wenchuan earthquake, the earthquake has a strong effect on the slope. The driving force of seismic intensity on the landslide spatial distribution was significantly higher than that of driving factors. In 2014, the driving force of the earthquake decreased, and the driving force of the rock mass increased significantly and replaced the dominant role of earthquake in the spatial distribution of the landslide. Although rock mass became the dominant factor controlled the spatial distribution of landslides in 2014, the role of the MS8.0 Wenchuan earthquake still cannot be ignored. Because the driving force of the earthquake was still stronger than that of the other driving factors except rock mass in 2014, which means the effects of the MS8.0 Wenchuan earthquake are still strong.

Under the joint effects some factors with weak driving forces have been significantly enhanced. As for individual driving forces, except for the driving forces of seismic intensity and rock mass are greater than 0.1, other driving factors are less than 0.1. When considering the joint effects of driving factors, it is found that except for the joint forces of Slope∩Roughness is still less than 0.1 (Fig. 5), the driving

forces of the other driving factors were all significantly enhanced due to the joint effects and all of them are greater than 0.1. Comparing the joint effects of driving factors in 2014 and 2009, the joint effects in 2014 are stronger than that of 2009 (except for DEM∩Residential), which reflects the fact that driving forces of driving factors on landslide spatial distribution have strengthened after 6 years of the MS 8.0 Wenchuan earthquake.

Compared with the joint effects among driving factors, there was a bigger difference in the joint effect between driving factors and earthquake in 2009 and 2014. The joint effects of earthquake are low in 2014 and high in 2009, but the joint effects of driving factors (except earthquake) are low in 2009 and high in 2014. It means that the changes of earthquake play an important role in driving the spatial distribution of landslides between 2009-2014. In addition, the joint effect of the earthquake is generally stronger than that of precipitation. It indicates that although 6 years since the MS 8.0 Wenchuan earthquake, the influence of the earthquake on spatial distribution of landslides is still higher than that of precipitation. As for the joint effects of precipitation, it did not have a certain pattern in 2009 and 2014, one possible reason is the spatial distribution of precipitation are randomly changed in 2009 and 2014.

Limitations exist in this study. First, the method used in this study only analyzed the driving force or joint effects of driving factors on the spatial distribution of landslides on a regional scale. When applying the relationship between driving

factors and landslides in this study on a local scale, it is necessary to combine more local environmental information for analysis. For example, the regional spatial distribution of the rainfall can't fully reflect the local rainfall intensity that may cause the driving force of intensive rainfall being underestimated. Second, though the results of two period data have revealed the joint effects and spatiotemporal characteristics of the landslide driving factors, if more periods of data are included the more details of spatiotemporal features can be provided. Third, the using kernel density map of landslide point to represent the spatial pattern of landslide may add some interpolation error, which may increase the uncertainties of the result. How to choose a better method to describe the spatial pattern of landslide needs further study.

The relationship between landslides and triggering factors or driving factors at the regional scale has been explored by many studies, providing insights on how the driving factors controlled the spatial distribution of landslides. However, few studies have revealed the joint effects of these factors. In this study, besides the driving forces of driving and triggering factors were detected, the joint effects of these factors were also considered. Moreover, the spatiotemporal characteristics of joint effects were further revealed. These more detailed findings help to develop targeted landslide prevention strategies.

5 Conclusion

This paper aimed to explore the joint effects and spatiotemporal characteristics of the driving factors of landslides in the MS8.0 Wenchuan earthquake area. From the

perspective of time, the landslide density in 2009 was significantly higher than that of 2014, and no matter in 2009 or 2014 the order of high-density to low-density of categories of each factor is consistent (except for factor rock mass). With regards to the individual driving force of a driving factor, factors with biggest driving forces in 2009 and 2014 are rock mass and seismic intensity, respectively. As for joint effects of driving factors, the joint effects of driving factors (except for the joint effects of DEM and residential area) in 2014 were stronger than in 2009. As for joint effects of driving factors and earthquake, the joint effects of earthquake and driving factors in 2009 were significantly stronger than that of 2014, and the joint effects of earthquake and rock mass rank the top. The driving force for the spatial distribution of landslides has been significantly enhanced under these joint effects. These joint effects and spatiotemporal characteristics can be used to identify the combinations that with a significant enhancement effect though comparing the joint effects and individual driving forces. Therefore, these results are helpful to understand the rules of how an earthquake action on secondary hazards.

ACKNOWLEDGMENT(S)

This research was funded by the National Natural Science Foundation of China, grant number 42071375; and the National Key Research and Development Program of China, grant number 2018YFC1504703-3. Thanks to professor Jinfeng Wang for his valuable guidance on this work and the free software Geodetector.

References

Achour, Y., Boumezbeur, A., Hadji, R., et al., 2017. Landslide susceptibility mapping using analytic hierarchy process and information value methods along a highway road section in Constantine, Algeria. *Arabian Journal of Geosciences*, 10(8)

Anis, Z., Wissem, G., Riheb, H., et al., 2019. Effects of clay properties in the landslides genesis in flysch massif: Case study of Ain Draham, North Western Tunisia. *Journal of African Earth Sciences*, 151: 146-152.

CEA (China Earthquake Administration), 2008. The Chinese seismic intensity scale. GB/T 17742-2008

Che, V. B., Kervyn, M., Ernst, G. G. J., et al., 2011. Systematic documentation of landslide events in Limbe area (Mt Cameroon Volcano, SW Cameroon): Geometry, controlling, and triggering factors. *Natural Hazards*,59(1): 47-74.

Cui, P., Wei, F. ,He, S., 2008. Mountain disasters induced by the earthquake of May 12 in Wenchuan and the disasters mitigation. *Journal of Mountain Science*, 26(3): 280-282. (in Chinese with English Abstract)

Dai, F. C., Lee, C. F. ,Ngai, Y. Y., 2002. Landslide risk assessment and management: an overview. *Engineering Geology*, 64(1): 65-87.

Fan, X., Zhang, Y. ,Yang, J. J. J. o. N. D., 2012. Developmental characteristics and influence factors of landslides in Wenchuan earthquake. *Journal of Natural Disasters*, 21(1): 128-134. (in Chinese with English Abstract)

Fan, X., Scaringi, G., Korup, O., et al., 2019. Earthquake-Induced Chains of Geologic Hazards: Patterns, Mechanisms, and Impacts. *Reviews of Geophysics*, 57(2): 421-503.

Furuichi, T., Osanai, N., Hayashi, S., et al., 2018. Disastrous sediment discharge due to typhoon-induced heavy rainfall over fossil periglacial catchments in western Tokachi, Hokkaido, northern Japan. *Landslides*, 15(8): 1645-1655.

Hadji, R., Boumazbeur, A. E., Limani, Y., et al., 2013. Geologic, topographic and climatic controls in landslide hazard assessment using GIS modeling: A case study of Souk Ahras region, NE Algeria. *Quaternary International*, 302: 224-237.

Hadji, R., Rais, K., Gadri, L., et al., 2017. Slope Failure Characteristics and Slope Movement Susceptibility Assessment Using GIS in a Medium Scale: A Case Study from Ouled Driss and Machroha Municipalities, Northeast Algeria. *Arabian Journal for Science and Engineering*, 42(1): 281-300.

Huang, R. Q., 2007. Large-scale landslides and their sliding mechanisms in China since the 20th century. *Chinese Journal of Rock Mechanics and Engineering*, 26: 433-454. (in Chinese with English Abstract)

Karim, Z., Hadji, R. ,Hamed, Y., 2018. GIS-Based Approaches for the Landslide Susceptibility Prediction in Setif Region (NE Algeria). *Geotechnical and Geological Engineering*, 37: 359–374.

Lee, S., Baek, W.-K., Jung, H.-S., et al., 2020. Susceptibility Mapping on Urban Landslides Using Deep Learning Approaches in Mt. Umyeon. *Applied Sciences-Basel*, 10(22)

Lin, C.W., Liu, S.H., Lee, S.-Y., et al., 2006. Impacts of the Chi-Chi earthquake on subsequent rainfall-induced landslides in central Taiwan. *Engineering Geology*, 86(2-3): 87-101.

Lin, C. W., Shieh, C. L., Yuan, B. D., et al., 2004. Impact of Chi-Chi earthquake on the occurrence of landslides and debris flows: example from the Chenyulan River watershed, Nantou, Taiwan. *Engineering Geology*, 71(1-2): 49-61.

Mahdadi, F., Boumezbeur, A., Hadji, R., et al., 2018. GIS-based landslide susceptibility assessment using statistical models: a case study from Souk Ahras province, N-E Algeria. *Arabian Journal of Geosciences*, 11(17)

Manchar, N., Benabbas, C., Hadji, R., et al., 2018. Landslide Susceptibility Assessment in Constantine Region (NE Algeria) By Means of Statistical Models. *Studia Geotechnica et Mechanica*, 40(3): 208-219.

Marano, K. D., Wald, D. J. ,Allen, T. I., 2010. Global earthquake casualties due to secondary effects: a quantitative analysis for improving rapid loss analyses. *Natural Hazards*, 52(2): 319-328.

Mendes, Rodolfo, M., et al., 2018. Understanding shallow landslides in Campos do Jordao municipality - Brazil: disentangling the anthropic effects from natural causes in the disaster of 2000. *Natural Hazards and Earth System Sciences*, 1: 15-30.

Pantelidis, L., 2011. A critical review of highway slope instability risk assessment systems. *Bulletin of Engineering Geology and the Environment*, 70(3): 395-400.

Persichillo, M. G., Bordoni, M., Cavalli, M., et al., 2018. The role of human activities on sediment connectivity of shallow landslides. *Catena*, 160: 261-274.

Shafique, M., van der Meijde, M. ,Khan, M. A., 2016. A review of the 2005 Kashmir earthquake-induced landslides; from a remote sensing prospective. *Journal of Asian Earth Sciences*, 118: 68-80.

Shafique, M., 2020. Spatial and temporal evolution of co-seismic landslides after the 2005 Kashmir earthquake. *Geomorphology*, 362.

Sheng, Y., 1959. Geomorphological Regionalization of China. Science Press, Beijing

Tang, C., Zhu, J., Li, W. L., et al., 2009. Rainfall-triggered debris flows following the Wenchuan earthquake. *Bulletin of Engineering Geology and the Environment*, 68(2): 187-194.

Tang, C., Zhu, J., Qi, X., et al., 2011. Landslides induced by the Wenchuan earthquake and the subsequent strong rainfall event: A case study in the Beichuan area of China. *Engineering Geology*, 122(1-2): 22-33.

Tang, Y. F., Wei.; Li, Zhenguo., 2015. A Review of the Study of Loess Slump. *Advance in Earth Sciences*, 30: 26-36.

Vargas-Cuervo, G., Rotigliano, E. ,Conoscenti, C., 2019. Prediction of debris-avalanches and -flows triggered by a tropical storm by using a stochastic approach: An application to the events occurred in Mocoa (Colombia) on 1 April 2017. *Geomorphology*, 339: 31-43.

Wang, G. L., Li, T. L., Xing, X. L., et al., 2015. Research on loess flow-slides induced by rainfall in July 2013 in Yan'an, NW China. *Environmental Earth Sciences*, 73(12): 7933-7944.

Wang, J. F. ,Hu, Y., 2012. Environmental health risk detection with GeogDetector. *Environmental Modelling & Software*, 33: 114-115.

Wang, J. F., Li, X. H., Christakos, G., et al., 2010. Geographical Detectors-Based Health Risk Assessment and its Application in the Neural Tube Defects Study of the Heshun Region, China. *International Journal of Geographical Information Science*, 24(1): 107-127.

Wang, J. F., Zhang, T. L. ,Fu, B. J., 2016. A measure of spatial stratified heterogeneity. *Ecological Indicators*, 67: 250-256.

Wang, J. F., Xu, C., 2017. Geodetector: Principle and prospective. *Acta Geographica Sinica*, 72(1): 116-134. (in Chinese with English Abstract)

Wang, Y., Lin, Q. G. ,Shi, P. J., 2018. Spatial pattern and influencing factors of landslide casualty events. *Journal of Geographical Sciences*, 28(3): 259-274.

Xu, C., Dai, F. C., Xu, X. W., et al., 2012. GIS-based support vector machine modeling of earthquake-triggered landslide susceptibility in the Jianjiang River watershed, China. *Geomorphology*, 145: 70-80.

Xu, C., Xu, X. W., Dai, F. C., et al., 2012. Comparison of different models for susceptibility mapping of earthquake triggered landslides related with the 2008 Wenchuan earthquake in China. *Computers & Geosciences*, 46: 317-329.

Xu, C., Xu, X., Shyu, J. B. H., et al., 2015. Landslides triggered by the 20 April 2013 Lushan, China, Mw 6.6 earthquake from field investigations and preliminary analyses. *Landslides*, 12(2): 365-385.

Xu, C., Xu, X. W., Shyu, J. B. H., 2015. Database and spatial distribution of landslides triggered by the Lushan, China Mw 6.6 earthquake of 20 April 2013. *Geomorphology*, 248: 77-92.

Xu, C., Xu, X., Shyu, J. B. H., et al., 2014. Landslides triggered by the 22 July 2013 Minxian-Zhangxian, China, Mw 5.9 earthquake: Inventory compiling and spatial distribution analysis. *Journal of Asian Earth Sciences*, 92(oct.): 125-142.

Xu, Q.,Huang, R., 2008. KINETICS CHARATERISTICS OF LARGE LANDLIDES TRIGGERED BY MAY 12TH WENCHUAN EARTHQUAKE. *Journal of Engineering Geology*, 16: 721-729. (in Chinese with English Abstract)

Xu, X., Xu, C., 2021. Natural Hazards Research: An eternal subject of human survival and development. *Natural Hazards Research*, 1: 1-3.

Yao, J., Qin, S., Qiao, S., et al., 2020. Assessment of Landslide Susceptibility Combining Deep Learning with Semi-Supervised Learning in Jiaohe County, Jilin Province, China. *Applied Sciences-Basel*, 10(16)

Yu, B., Yang, L., Chang, M., et al., 2021. A new prediction model on debris flows caused by runoff mechanism. *Environmental Earth Sciences*, 80(1)

Chen, Y., Yu, B., Zhu, Y., et al., 2013. Variation characteristics of debris flow critical rainfall after an earthquake-Taking Xiaogangjiangou in Wenchuan earthquake area as an example. *Journal of Mountain Science*(3): 102-107. (in Chinese with English Abstract)

Zhao, Q., Wang, Y., Cao, Y., et al., 2014. Potential health risks of heavy metals in cultivated topsoil and grain, including correlations with human primary liver, lung and gastric cancer, in Anhui province, Eastern China. *Science of the Total Environment*, 470: 340-347.

List of Tables

Table 1. Names, data structures, types, descriptions and factor type of influencing factors.

Variables	Name	Data structure	Variable type	Data description	Category
Y	Landslide Point	Point	Frequency	The number of landslide points in each grid in 2009 and 2014.	Landslide
X1	Seismic Intensity	Polygon	Discrete	The seismic intensity of the 2008 MS 8.0 Wenchuan earthquake	Triggering factor
X2	Precipitation	Polygon	Discrete	Annual average precipitation classification in 2009 and 2014.	Triggering factor
X3	Rock Mass	Polygon	Discrete	The hardness of the rock and soil	Driving factor
X4	Elevation	Raster	Continuous	Digital elevation model	Driving factor
X5	Roughness	Raster	Continuous	The roughness index of terrain	Driving factor
X6	Slope	Raster	Continuous	Extracted from DEM	Driving factor
X7	Road	Line	Continuous	Distance to road	Driving factor
X8	Residential area	Point	Continuous	Distance to point	Driving factor

Figure legends

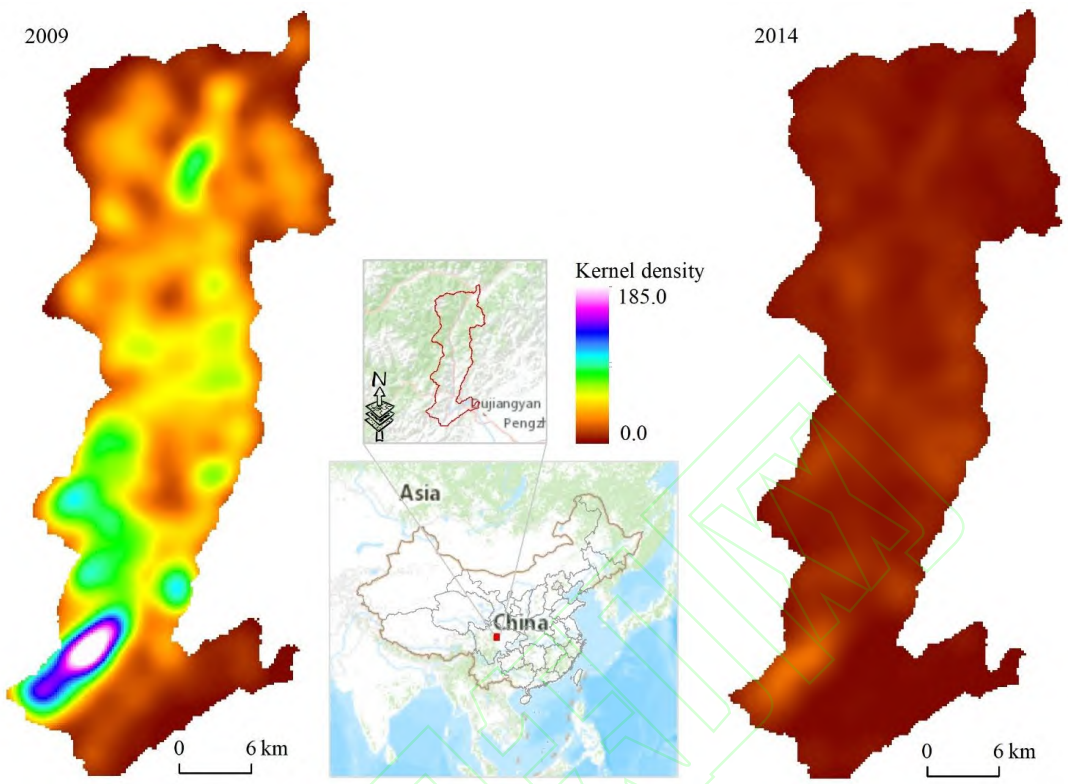

Figure 1. Maps showing location of study area and the kernel density of landslide points in 2009 and 2014.

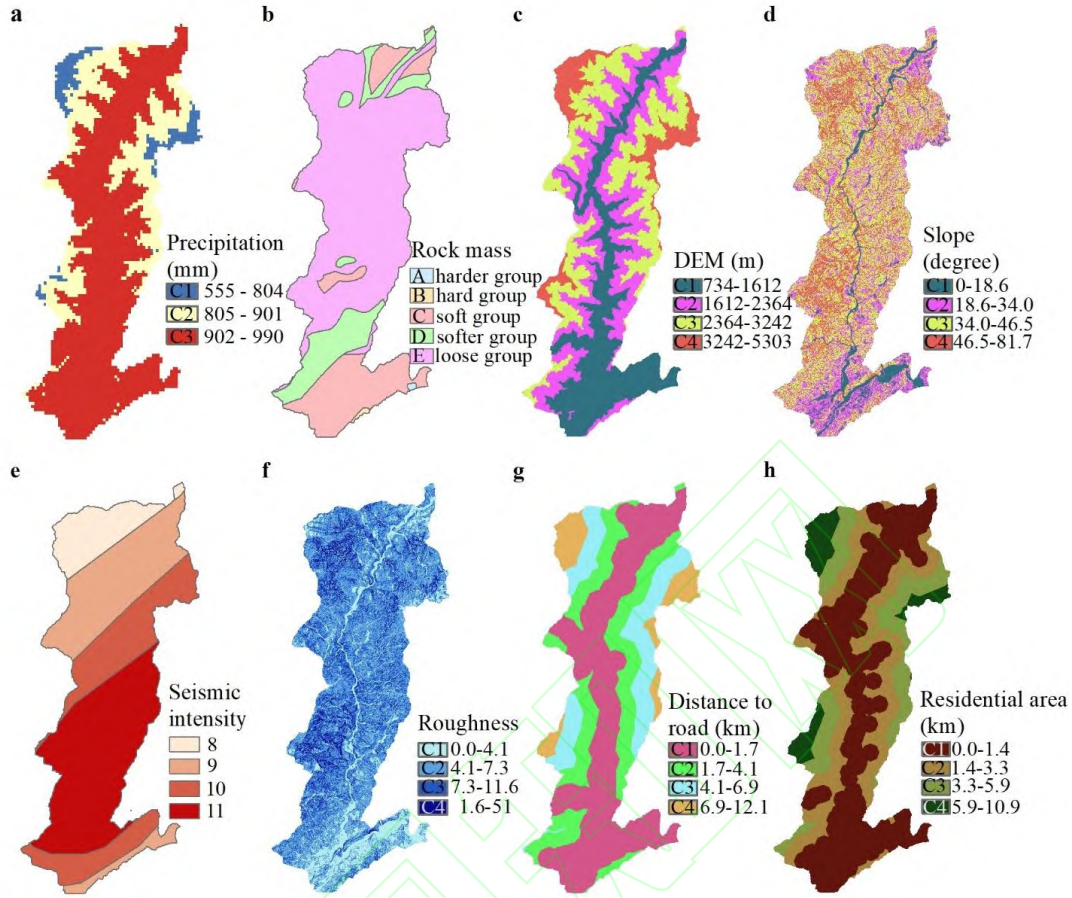

Figure 2. Thematic maps of condition factors. (a) Annual average precipitation in 2014, (b) Rock Mass, (c) Digital elevation model, (d) Slope, (e) The seismic intensity of the MS 8.0 Wenchuan earthquake, (f) The roughness index of terrain, (g) The distance to road, and (h) the distance to residential area.

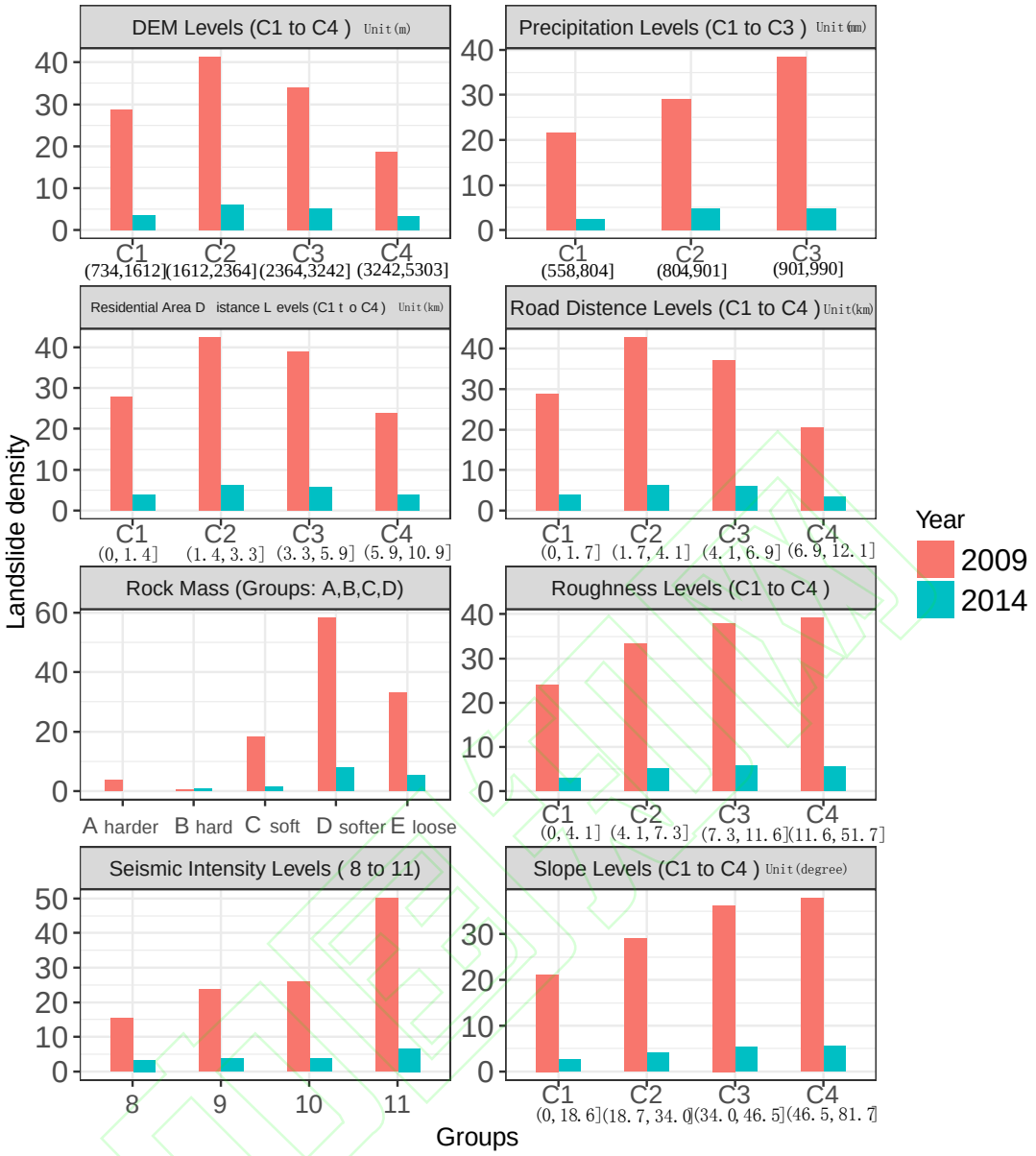

Figure 3. The distribution of landslide density values under different geographic conditions in 2009 and 2014.

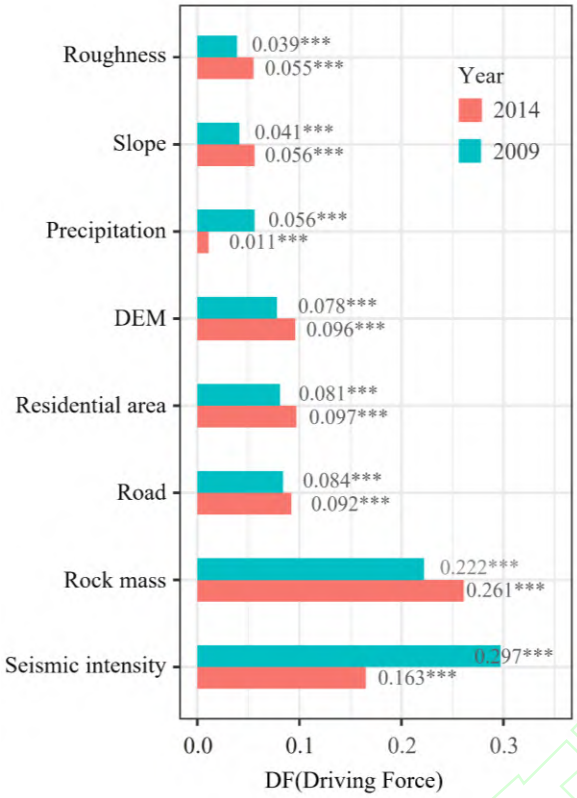

Figure 4. The driving force of driving factors to the spatial distribution of landslides in 2009 and 2014.

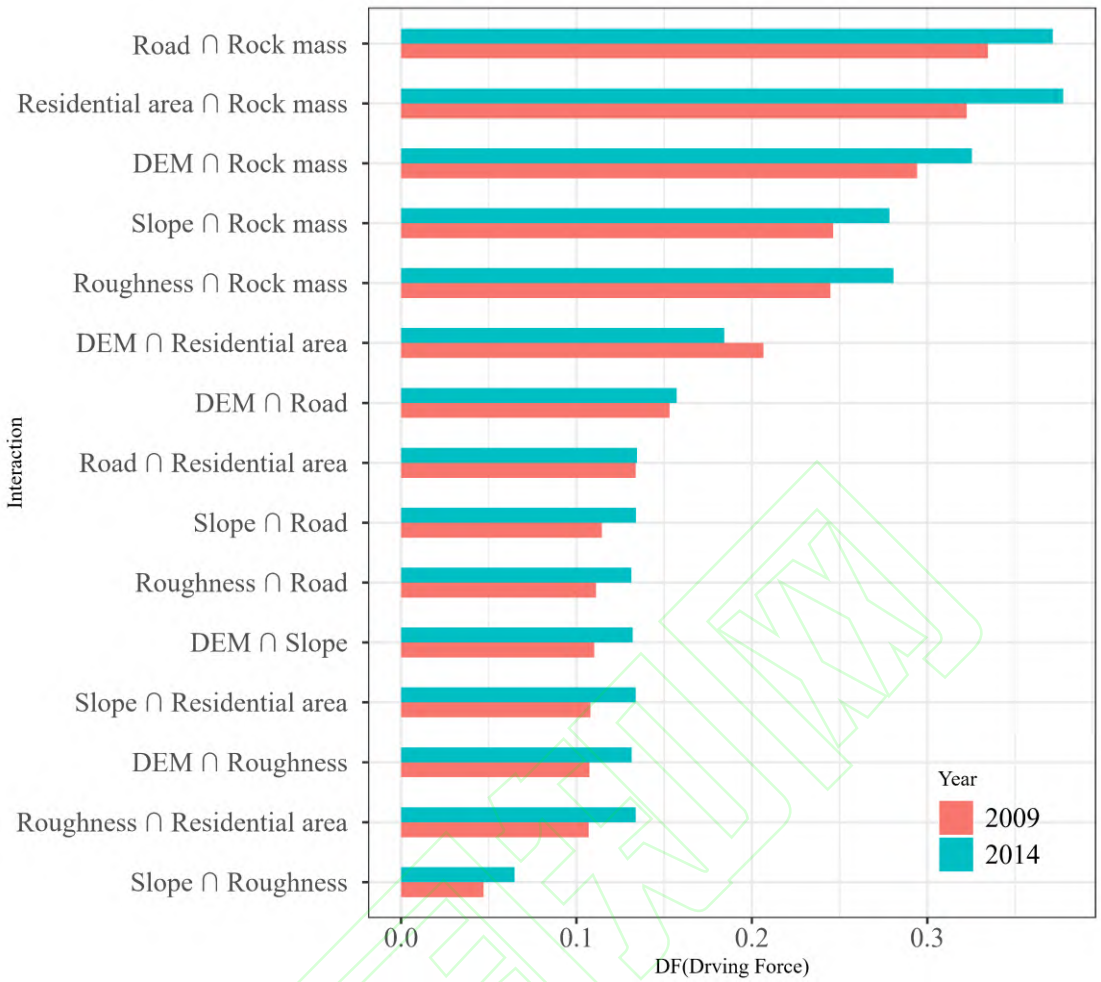

Figure 5. The joint effect of driving factors on landslide spatial distribution in 2009 and 2014. (Symbol ∩ represents the joint-effect, e.g A∩B represents the joint effect of A and B)

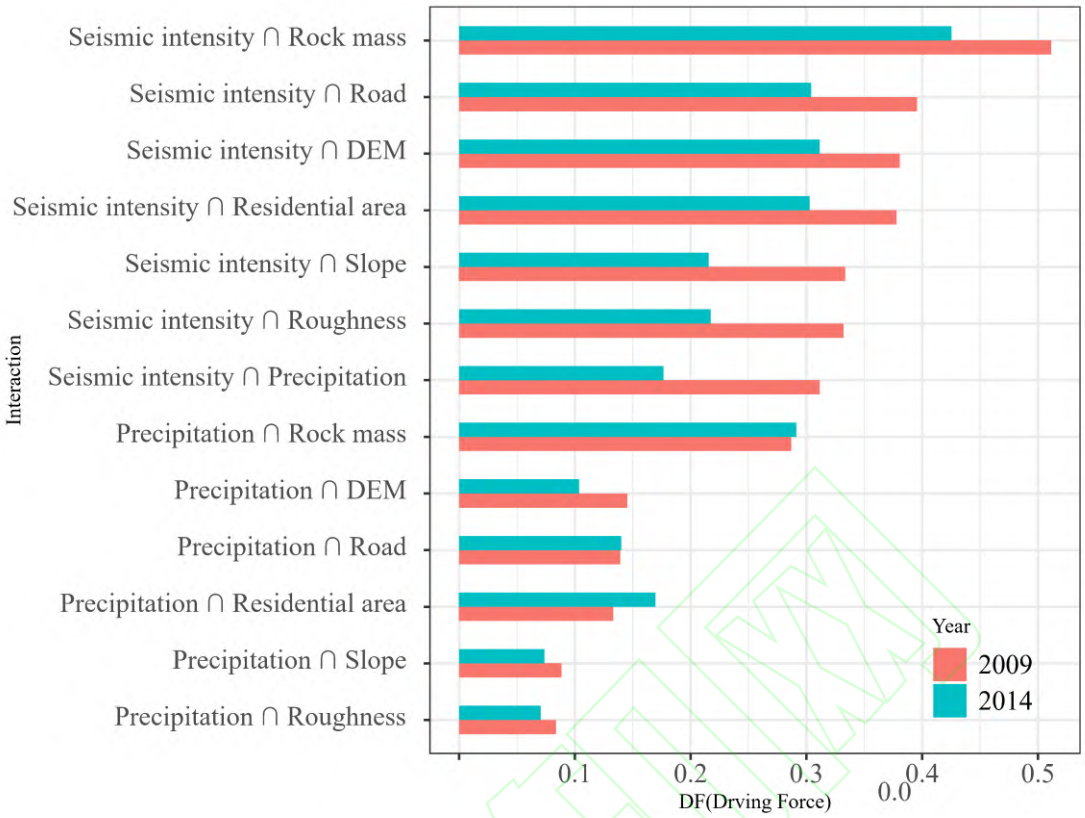

Figure 6. The joint effect of driving factor and triggering factor on landslide spatial distribution in 2009 and 2014. (symbol ∩ represents the joint-effect, e.g A∩B represents the joint effect of A and B)